GLOWA Jordan River

High resolution climate scenarios for the Near East

Andreas Heckl, Patrick Laux, Peter Suppan, Harald Kunstmann,
Institute for Meteorology and Climate Research, IMK-IFU, Germany

Problem:
Changes in the regional climate can differ significantly from the overall trend of global climate change
Region has sharp climatic gradients: subhumid mediterranean ⇔ arid climate
Resolution of global climate models are much too coarse for further regional studies about climate impact
→ High resolution information required that account for regional and local geographic features (particularly orography, land use and water bodies)

Solution: Dynamic downscaling of global climate scenarios

Methodology and current status:
Explicit dynamical downscaling of global meteorological fields with MM5
Three nesting steps (grid size of 54, 18, 6km)
25 vertical levels
Control run CT (1961-1990) and scenarios A2 & B2 from GCM ECHAM4
- Control run and scenario B2 (2070-2099) finished for domain 2
- Control run finished for Domain 3 (1961-1975), scenario B2 in progress
- transient runs with scenarios A2 + B2 finished for Domain 1 (1961-2050), domain2 in progress

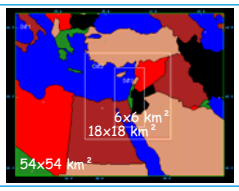

Fig. 1: Location of the three Domains and their respective resolution

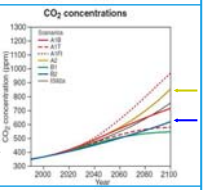

Fig. 2: Changes in theCO2-concentrations for the different IPCC-scenarios, Selected Scenarios: A2 (more pessimistic) and B2 (more optimistic)

Results:

1) Mean annual climate changes

Figure 3 shows that till 2050 the different scenarios don't offer big differences: in both cases they expose an increase of yearly temperatures of 1.5 – 2 K. The same can be seen in Figure 4 with the mean annual precipitation: both scenarios have little increases in the northern parts and decreases in in the south. In scenario B2 instead happens till the end of the century (2070-2099) an extreme reduction of precipitation amounts all over the region.

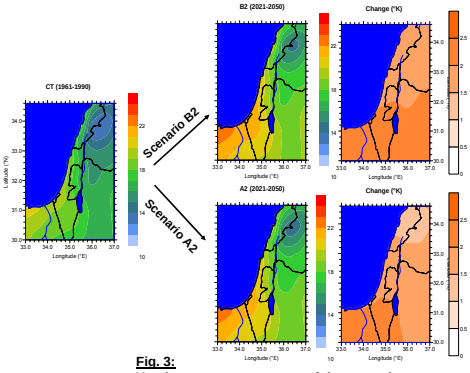

Fig. 3: Yearly mean temperatures of the control run, the future scenarios A2 + B2 (2021-2050) and changes

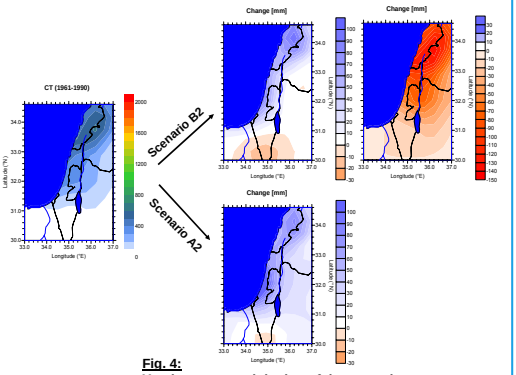

Fig. 4: Yearly mean precipitation of the control run and future changes for the scenarios A2 + B2

2) Regional and seasonal changes

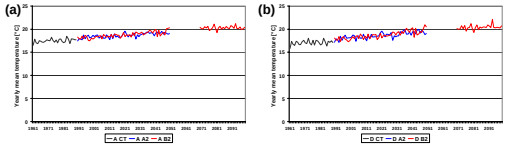

Fig. 6: Yearly mean temperatures for regions A (a) and D (b)

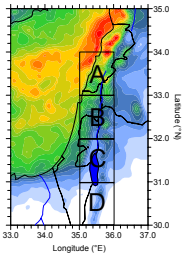

Fig. 5: Region divided into four areas A-D to detect regional differences

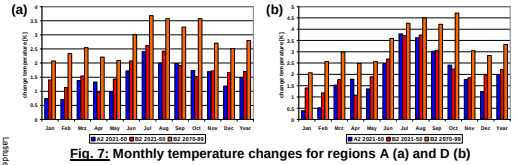

Fig. 7: Monthly temperature changes for regions A (a) and D (b)

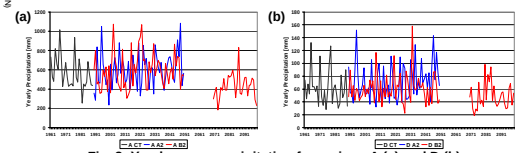

Fig. 8: Yearly mean precipitation for regions A (a) and D (b)

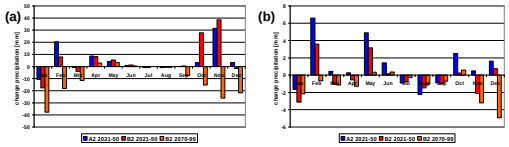

Fig. 9: Monthly precipitation changes for regions A (a) and D (b)

Figure 6 shows steadily increasing annual mean temperatures with little variability in both scenarios. Differences in monthly temperature changes are mostly little between the scenarios in 2021-2050 (Figure 7), but more significant in monthly precipitation changes (Figure 9). High variability in precipitation can be seen in Figure 8 with no clear trend till 2050, but strongly decreasing rain amounts for the later time slice (2070-2099).

3) Changes in extremes

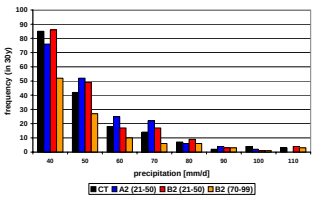

Fig. 10: Changes in heavy precipitation frequency

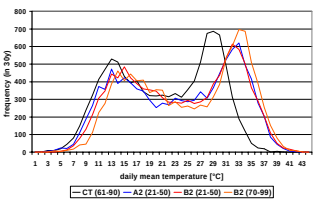

Fig. 11: Changes in frequency of temperatures (daily mean)

Fig. 10 shows the expected changes in the frequencies of the extreme precipitation events in dependence of greenhouse gas emission scenario and time slice. For the daily mean temperature (Figure 11), a clear shift towards higher temperatures is expected in the future.

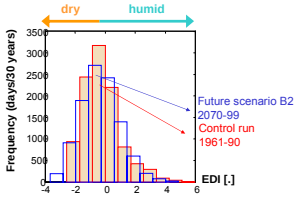

Fig. 12: Frequencies of EDI for the control run and the future scenario B2

The effective drought index (EDI) was determined for the control run (1961-90) and the scenario B2 (2070-99) in 18km resolution (example for region A, see Figure 5). Figure 12 shows the change of EDI-frequencies for scenario B2 compared to the baseline period. Very dry situations will increase in the future (EDI < -2).
Figure 14 is displaying the relationship between drought intensity and drought duration. Strong Pearson correlation (r) coefficients are found. For the big drought events, the functions are converging. Higher drought intensities can be found for the future (Figure 14b) than for the control run (Figure 14a).

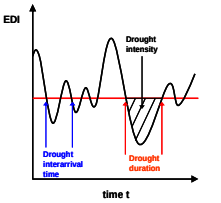

Fig. 13: Explanation of drought intensity and drought duration

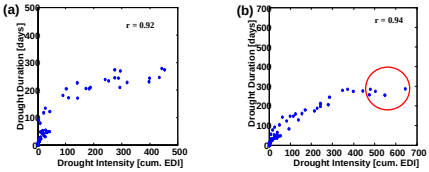

Fig. 14: Relationship between drought intensity and drought duration for the control run (a) and the future scenario B2 (b)

Outlook for phase III:
- Finishing transient runs in 18 km resolution
- Extension of set of simulations with two other GCM: ECHAM5 and HadCM3 (also transient 1961-2050, scenario A1B, 54km and 18km resolution) to detect uncertainties coming from the regional (MM5 ⇔ RegCM of TAU) and the global models (ECHAM5 ⇔ HadCM3)
- Objective circulation pattern analysis for regional refinement of rainfall distribution
  - ➢ Identification of wet and dry circulation patterns (CPs) (Figure 15)
  - ➢ Stochastic conditional rainfall modeling (daily and site scale)
  - ➢ Frequency analysis (scenarios vs. control run) (Figure 16)

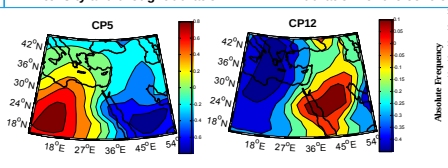

Fig. 15: Example of wet (CP5) and dry (CP12) circulation pattern (anomaly composites) based on *sea level pressure* for the control run (1961-1990)

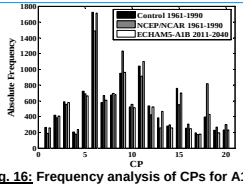

Fig. 16: Frequency analysis of CPs for A1B (2011-2040) compared to NCEP/NCAR and ECHAM5 control run (1961-1990)

Contact: Andreas Heckl, Forschungszentrum Karlsruhe, 82467 Garmisch-Partenkirchen, Germany
andreas.heckl@imk.fzk.de